Modeling Gradient Elution of Proteins in Ion-Exchange Chromatography

Stuart R. Gallant
Bayer Corporation, 800 Dwight Way, B56B, Berkeley, CA 94701

Suresh Vunnum and Steven M. Cramer
Howard P. Isermann Dept. of Chemical Engineering, Rensselear Polytechnic Institute, Troy, NY 12180

The steric mass action (SMA) model of ion exchange is employed in concert with appropriate mass balance equations to describe the behavior of a concentrated band of protein under gradient-elution conditions. A method of characteristics approach is employed to solve the model equations rapidly. The model is shown to accurately predict the gradient elution of the protein cytochrome C in a strong cation-exchange column. This work constitutes an advance over previously available models as it allows engineers to rapidly consider the effects of nonlinear adsorption in gradient-elution chromatography using a spreadsheet. Further, it provides significant physical insight into the process of gradient elution for preparative and large-scale separations.

Introduction

Gradient elution is frequently used in both analytical and preparative chromatography for separation of biological feed streams. In analytical chromatography, a relatively small mass of the sample is loaded onto the chromatographic column. Since the resulting chromatographic bands have relatively low concentration, the forces of dispersion (Taylor dispersion, eddy dispersion, and film and pore mass transport resistances) control the band shape (Gibbs and Lightfoot, 1986; Frey, 1990; Carta and Stringfield, 1992). In contrast, preparative injections often involve substantial loadings that may occupy 25% or more of the column length during the feed cycle. During elution, high mobile-phase concentrations of the feed components often result in nonlinear adsorption and competitive binding.

To model gradient elution under conditions of infinite dilution (analytical chromatography), the linear solvent strength theory (LSS) has been developed (Snyder, 1980; Parente and Wetlaufer, 1986; Yamamoto et al., 1987). LSS predicts the retention time of a chromatographic band in the linear or Henry's law region of the adsorption isotherm. Subsequent researchers have developed models that include dispersion forces and allow the shape of the chromatographic band to be predicted under dilute conditions (Gibbs and Lightfoot, 1986; Frey, 1990; Carta and Stringfield, 1992). However, the assumption of Henry's law adsorption is often not valid in preparative gradient chromatography. During the feed stage, the stationary-phase concentration becomes quite large, even for dilute feed streams. As the gradient strength increases during elution, nonlinear adsorption can lead to shock formation and "shark fin" shaped chromatographic bands.

Protein adsorption in ion exchange has been considered by a number of authors. Stoichiometric exchange (Boardman and Partridge, 1955; Helfferich and Klein, 1970) has been utilized by Regnier and coworkers to model protein adsorption under conditions of infinite dilution (Drager and Regnier, 1986). At higher protein concentrations, the finite capacity of the stationary phase (Velayudhan and Horváth, 1988) and the blockage or steric shielding of the stationary-phase surface by biopolymers play important roles in equilibrium adsorption. Whitley et al. (1989) have developed a method for addressing the steric shielding phenomena in binding of a single protein at high concentration. Li and Pinto (1994) have developed a method for addressing nonideal protein adsorption based on UNIQUAC, which accounts for protein–protein interactions on the chromatographic surface. Significantly, Velayudhan (1990) observed that the number of blocked sites is proportional to the adsorbed protein concentration. Brooks and Cramer (1992) used this insight as the basis of the steric mass action (SMA) formalism. Subsequently, SMA has been shown

Correspondence concerning this article should be addressed to S. M. Cramer.

capable of representing linear and multicomponent nonlinear adsorption of proteins and polyelectrolytes over a wide range of operating conditions commonly encountered in preparative chromatography (Gerstner and Cramer, 1992a,b; Gadam et al., 1993, 1995; Jayaraman et al., 1993; Gallant et al., 1995a,b, 1996).

The problem of adsorption described by the Langmuir and other constant separation factor isotherms has been studied quite extensively, and a number of analytical solutions have been presented (Helfferich and Klein, 1970; Rhee et al., 1986). However, for most other isotherms, investigators have resorted to numerical methods for solution of the mass transport and adsorption equations describing chromatography (Yamamoto et al., 1983a,b; Antia and Horváth, 1989; Czok and Guichon, 1990a,b; Snyder et al., 1991; Ma and Guichon, 1991; Gu et al., 1992; Bellot and Condoret, 1993; Whitley et al., 1994). However, the use of a nonconstant separation factor isotherm does not, in itself, prevent an analytical solution of a given problem, even if that isotherm is nonlinear. In this article, the elution of a chromatographic band of finite width and concentration in gradient ion-exchange chromatography is considered. The isotherm is the nonconstant separation factor SMA isotherm, and substantial nonlinearity is present; the solution of this problem employs the method of characteristics. This approach leads to a simple model that can be rapidly solved utilizing a spreadsheet.

Theory

Equilibrium formalism

The SMA formalism is a three-parameter model of ion exchange designed specifically for representation of multicomponent protein–salt equilibrium in ion-exchange chromatography (Brooks and Cramer, 1992). The protein is bound to the stationary phase at a number of exchange sites given by its *characteristic charge*, ν_i. In addition, binding of the protein sterically shields or blocks a number of sites given by its *steric factor*, σ_i. Finally, the equilibrium of the exchange process is represented by an *equilibrium constant*, K_{1i}.

The equilibrium constant of the reaction may be written

$$K_{1i} = \left(\frac{Q_i}{C_i}\right)\left(\frac{C_1}{\bar{Q}_1}\right)^{\nu_i} \qquad i = 2, \ldots, NC, \tag{1}$$

where C_i and Q_i refer to the concentration of protein in the mobile phase and on the stationary phase, C_1 refers to the concentration of salt in the mobile phase, and $\bar{Q}_1$ refers to the concentration of bound salt available for exchange.

Each protein molecule may sterically shield some salt counterions on the adsorptive surface. The quantity of salt counterions blocked by a particular protein will be proportional to the concentration of that protein on the surface:

$$\hat{Q}_{1i} = \sigma_i Q_i \qquad i = 2, \ldots, NC. \tag{2}$$

Electroneutrality requires that

$$\Lambda = \bar{Q}_1 + \sum_{i=2}^{NC} (\nu_i + \sigma_i) Q_i. \tag{3}$$

Field equations and boundary conditions

In an ideal model of chromatography, convective transport is taken as the dominant phenomenon and dispersion is disregarded. Transport within the column is described by the following system of partial differential equations (Wankat, 1990; de Bokx et al., 1992):

$$\frac{\partial C_i}{\partial x} + \frac{\partial C_i}{\partial \tau} + \beta \frac{\partial Q_i}{\partial \tau} = 0 \qquad i = 1, \ldots, NC, \tag{4}$$

where β is a phase ratio, x is nondimensional measure of the axial position ($x = X/L$), and τ is a dimensionless time unit ($\tau = t/t_0$). In these nondimensional coordinates, the velocity of an unretained component in the mobile phase is one. Retained components will have velocities less than one.

In linear gradient chromatography, the salt concentration is a ramp function at the column inlet:

$$C_1(\tau \le \tau_f, 0) = C_{1,f} \tag{5a}$$

$$C_1(\tau > \tau_f, 0) = C_{1,f} + [G_{\text{slope}} * (\tau - \tau_f)], \tag{5b}$$

where τ_f is the length of the feed pulse and G_{slope} is the gradient slope. The feed stream is loaded and subsequently eluted:

$$C_2(0 < \tau < \tau_f, 0) = C_{2,f} \quad \text{(Loading)} \tag{6a}$$

$$C_2(\tau > \tau_f, 0) = 0 \quad \text{(Elution)}. \tag{6b}$$

In this problem, only the elution of a single protein is considered. The limitations of that approach will be addressed below.

The total concentration of components 1 and 2 (counterion and protein) given in equivalents constitutes a third variable, C_T:

$$C_T(\tau < 0, 0) = C_{1,f} \tag{7a}$$

$$C_T(0 < \tau < \tau_f, 0) = C_{1,f} + \nu_2 C_{2,f} \tag{7b}$$

$$C_T(\tau > \tau_f, 0) = C_{1,f} + [G_{\text{slope}} * (\tau - \tau_f)]. \tag{7c}$$

Because the adsorption of protein results in the displacement of a number of counterions equivalent to the characteristic charge of the protein, ν_2, the disturbances of C_T due to the feed injection and the salt gradient propagate through the column at the mobile-phase velocity:

$$C_T(\tau, x) = C_T(\tau - x, 0). \tag{8}$$

As a result, the total equivalents of protein and counterion at any point in the column and at any time may be calculated based solely on the boundary conditions. Knowledge of the behavior of C_T throughout the solution will play an important role in facilitating the solution of this problem.

Solution of the model

The preceding field and boundary conditions may be solved in conjunction with the SMA isotherm to produce an ideal

chromatogram. The procedure that will be employed in this work utilizes the method of characteristics (Hildebrand, 1976; Rhee et al., 1986). The assumptions of the model include:

1. The field equations of ideal chromatography govern mass transport.
2. The SMA isotherm governs protein adsorption.
3. The characteristic charge of the protein may be represented by an integer.
4. The salt concentration in the gradient $C_1(\tau, x)$ for $\tau - x > \tau_f$ may be approximated by the total equivalents $C_T(\tau, x)$.

The first two assumptions have already been discussed. The third assumption is significant because an integral characteristic charge permits an analytical result. As will be seen below, this assumption does not place a significant restriction on the solution because fractional characteristic charges may be represented by the nearest integer. For example, a protein possessing a characteristic charge (ν_i) of 3.3 may be taken to have a characteristic charge of 3.0 provided that the equilibrium constant (K_{1i}) and steric factor (ν_i) are revisited to establish values of these two parameters that provide the best fit to the experimental data based on the new characteristic charge.

The validity of the final assumption depends on the concentration of protein involved and on the characteristic charge of the protein. If the protein involved has a characteristic charge of 6.0 (e.g., cytochrome C, which is discussed), a relatively high mobile-phase concentration of 0.2 mM will result in an error in salt concentration (C_1) of 1.2 mM. Since a gradient will typically range over more than 100 mM in counterion concentration, this approximation has a small impact on the final solution.

The solution will proceed in eight steps, which are described below. On the basis of this description, this model may be implemented in a computer program or, more conveniently, in a computer spreadsheet.

Calculation of the Zones of C_T. As mentioned earlier in the discussion of Eq. 8, the value of C_T may be calculated at any point in the solution based on the boundary conditions. The representation of C_T in the time-space plane (i.e., in a development plot) forms three zones. In Figure 1, the first zone is labeled "Zone I" and constitutes all of the space below the bottom dotted line (slope = 1 and time-axis intercept = 0). In this region, the equilibration buffer perfuses the column: $C_T = C_1 = C_{1,f}$.

In Figure 1, the second zone is labeled "Zone II" and constitutes the space above Zone I and below the second dotted line (slope = 1 and time-axis intercept = τ_f). In this region, the total equivalents are given by the equivalents of protein and salt in the feed: $C_T = C_{1,f} + \nu_2 C_{2,f}$. The final zone above the second dotted line, "Zone III" in Figure 1 where $\tau - x > \tau_f$, is the region in which the gradient begins to increase:

$$C_T(\tau, x) = C_{1,f} + [G_{\text{slope}} * (\tau - x - \tau_f)]. \tag{9}$$

Calculation of Initial Frontal Protein and Salt Concentrations. During the loading cycle, a front of protein proceeds through the chromatographic column. Since the mobile-phase protein ($C_{2,f}$) and salt ($C_{1,f}$) concentrations are known from the boundary conditions, calculation of the bound protein and salt concentrations involves a simple equilibrium calculation

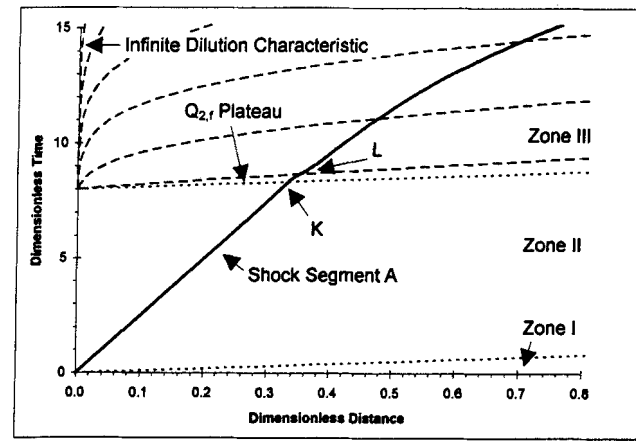

Figure 1. Development plot for gradient chromatography (close-up).

Simulated gradient elution of protein cytochrome C. Feed Injection: 8.0 dimensionless time units of 0.2-mM cytochrome C in 30-mM sodium phosphate, pH 6.0. Gradient Slope: 10-mM sodium ion concentration per dimensionless time unit. Plot includes changes in the value of C_T (dotted lines), the protein front or "shock" (dark solid line), and characteristics of the tail (dashed lines). This figure represents an expanded view of one region of Figure 2.

using the SMA isotherm, Eqs. 1–3. The bound protein and salt concentrations will be designated $Q_{2,f}$ and $Q_{1,f}$.

Calculation of Shock during Feed Cycle. The front of protein moves at a constant velocity during the loading cycle. In Figure 1, this front or "shock" is represented by a straight line that originates at the point (0,0) and follows the equation:

$$\tau = \left(1 + \beta \frac{Q_{2,f}}{C_{2,f}}\right) x, \tag{10}$$

where $C_{2,f}$ and $Q_{2,f}$ are the mobile- and stationary-phase concentrations of protein behind the shock.

Since the protein is adsorbed during the loading cycle, the shock travels slower than the mobile-phase velocity. As a result, the second disturbance in total equivalents C_T catches up with the shock. The point at which the shock and the disturbance in total ion concentration due to the end of the feed slug intersect is designated as point K in Figure 1.

Calculation of Bound Protein Concentration above the Disturbance in C_T. The second disturbance in total ion concentration C_T (the upper dotted line in Figure 1) travels at the nondimensional mobile phase velocity ($u_T = 1$). This discontinuous change or shock in C_T is itself made up of discontinuous changes or shocks in mobile phase protein and salt concentrations. The velocity of any discontinuity within the column is given by the expression

$$u_{sh} = \frac{1}{1 + \beta \dfrac{\Delta Q_i}{\Delta C_i}} \qquad i = 1 \text{ and } 2. \tag{11}$$

Since the discontinuity in C_T moves through the column with velocity of one ($u_{sh} = u_T = 1$), it can be seen that ($\Delta Q_i / \Delta C_i$)

$= 0$. Thus, the *bound* concentrations of protein and salt do not change across the discontinuity caused by the change in C_T, and are known to be $Q_{2,f}$ and $Q_{1,f}$ in the region just above the discontinuity.

Calculation of the Infinite Dilution Elution Point. Based on continuity considerations, the concentration velocity of any component is given by the equation (Helfferich and Klein, 1970)

$$u_{c,i} = \frac{1}{1 + \beta \dfrac{\partial Q_i}{\partial C_i}} \qquad i = 1 \text{ and } 2. \tag{12}$$

For the protein, Eq. 12 may be written

$$\frac{d\tau}{dx} = 1 + \beta \frac{\partial Q_2}{\partial C_2}. \tag{13}$$

When Eq. 13 is evaluated at an arbitrary constant protein concentration, a characteristic equation results. This equation defines the path of an arbitrary concentration through the solution plane.

Snyder and coworkers' linear solvent strength theory may be employed to establish the point at which the chromatographic peak finishes eluting from the column (Snyder, 1980). Under conditions of infinite dilution with respect to protein ($C_2 \approx 0$) for SMA equilibrium:

$$\frac{d\tau}{dx} = 1 + \beta K_{12} \left(\frac{\Lambda}{C_1} \right)^{\nu_2}. \tag{14}$$

Since protein concentration is negligible ($C_2 \approx 0$), the counterion concentration is known analytically ($C_1 = C_T$). Substituting Eq. 9 into Eq. 14:

$$\frac{d\tau}{dx} = 1 + \beta K_{12} \left(\frac{\Lambda}{C_{1,f} + G(\tau - x - \tau_f)} \right)^{\nu_2}. \tag{15}$$

Now substituting the variable $\tau^* = \tau - x - \tau_f$:

$$\frac{d\tau^*}{dx} = \beta K_{12} \left(\frac{\Lambda}{C_{1,f} + G\tau^*} \right)^{\nu_2}. \tag{16}$$

The integral may be written:

$$\int_0^{\tau^*} (C_{1,f} + Gy)^{\nu_2} dy = \int_0^x \beta K_{12} \Lambda^{\nu_2} dw, \tag{17}$$

where w and y are dummy variables of integration. The solution is

$$\tau^* = \frac{\left((\nu_2 + 1) G \beta K_{12} \Lambda^{\nu_2} x + C_{1,f}^{\nu_2 + 1} \right)^{1/(\nu_2 + 1)} - C_{1,f}}{G}. \tag{18}$$

Transforming the integral back into the original coordinates:

$$\tau = \frac{\left((\nu_2 + 1) G \beta K_{12} \Lambda^{\nu_2} x + C_{1,f}^{\nu_2 + 1} \right)^{1/(\nu_2 + 1)} - C_{1,f}}{G} + x + \tau_f. \tag{19}$$

This line, the infinite dilution characteristic, is depicted as the highest (i.e., slowest) dashed line in Figure 1. Any protein concentration greater than infinite dilution ($C_2 > 0$) will emerge from the column earlier than this characteristic.

Calculation of the Tail. In order to establish the shape of the chromatographic peak as it elutes from the column, characteristics of finite concentration must be calculated. Again, the concentration velocity (Eq. 13) equation is employed. However, the partial derivative is now calculated for a finite protein concentration in a two-component system (protein and salt) using the SMA isotherm:

$$\frac{d\tau}{dx} = 1 + \beta \frac{\dfrac{Q_2}{C_2} + \nu_2^2 \dfrac{Q_2}{C_1}}{1 - \nu_2 + \nu_2 \dfrac{\Lambda}{\overline{Q}_1}}. \tag{20}$$

In this case, it is desirable to follow characteristics of constant bound protein concentration Q_2. As a result, the concentration of bound salt available for exchange $\overline{Q}_1$ may also be taken as constant along a given characteristic. The integral may be written:

$$\int_0^{\tau^*} \frac{dy}{\dfrac{Q_2}{C_2} + \nu_2^2 \dfrac{Q_2}{C_1}} = \int_0^x \frac{\beta \, dw}{1 - \nu_2 + \nu_2 \dfrac{\Lambda}{\overline{Q}_1}} \tag{21}$$

or

$$\int_0^{\tau^*} \frac{dy}{A \left(\dfrac{1}{C_1} \right)^{\nu_2} + \dfrac{B}{C_1}} = \int_0^x D \, dw, \tag{22}$$

where w and y are dummy variables of integration, and the following quantities are constant along a given characteristic:

$$A = K_{12} \overline{Q}_1^{\nu_2} \tag{23a}$$

$$B = \nu_2^2 Q_2 \tag{23b}$$

$$D = \frac{\beta}{1 - \nu_2 + \nu_2 \dfrac{\Lambda}{\overline{Q}_1}}. \tag{23c}$$

It is expected that A will be significantly larger than B for realistic problems.

In order to allow a solution, the mobile-phase salt concentration will be approximated by the total ion concentration C_T, which is known through Eq. 9:

$$\int_0^{\tau^*} \frac{dy}{A\left(\frac{1}{C_{1,f}+Gy}\right)^{\nu_2}+\frac{B}{C_{1,f}+Gy}} = \int_0^x D\,dw \qquad (24)$$

or

$$\left[\left(\frac{1}{GB}\right)\left(\frac{B}{A}\right)^{2/(1-\nu_2)}\right]\left[\int_{(A/B)^{1/(1-\nu_2)}C_{1,f}}^{(A/B)^{1/(1-\nu_2)}(C_{1,f}+\tau^*G)} \frac{y\,dy}{y^{(1-\nu_2)}+1}\right] = \int_0^x D\,dw, \qquad (25)$$

where $\tau^* = \tau - x - \tau_f$. In Table 1, the solution to the integral on the lefthand side is given for various integral values of characteristic charge. Using this integral, the characteristics can be evaluated in three ways:

1. Fixed values of τ^* may be substituted into the solution of Eq. 25 allowing x to be calculated explicitly for a given value of Q_2: $x = \Xi(\tau^*, Q_2)$. Subsequently, τ is calculated: $\tau = \tau^* + \Xi(\tau^*, Q_2) + \tau_f$. (It may not readily be apparent why $\Xi(\tau^*, Q_2)$ is a function of two variables until it is recalled that the constants A and D are themselves functions of protein concentration.)

2. Fixed values of x may be substituted into the solution of Eq. 25 allowing τ^* to be calculated implicitly using a Newton–Raphson method for a given value of Q_2: $\tau^* = T^*(x, Q_2)$. Subsequently, τ is calculated: $\tau = T^*(x, Q_2) + x + \tau_f$.

3. Fixed values of x and τ may be substituted into the solution of Eq. 25 allowing Q_2 to be calculated implicitly using a Newton–Raphson method: $Q_2 = \Theta(\tau, x)$.

Table 1. Table of Integrals for Eq. 25

n	$\int \frac{x\,dx}{x^{(1-n)}+1}$
2	$\frac{x^2}{2} - x + \ln(x+1) + \text{const.}$
3	$\frac{x^2 - \ln(x^2+1)}{2} + \text{const.}$
4	$\frac{x^2}{2} + \frac{\ln(x+1) - \frac{\ln(x^2-x+1)}{2} - \sqrt{3}\arctan\left(\frac{2x-1}{\sqrt{3}}\right)}{3} + \text{const.}$
5	$\frac{x^2 - \arctan(x^2)}{2} + \text{const.}$
6	$\frac{x^2}{2} + \frac{\ln(x+1)}{5} + \left(\frac{\sqrt{5}-1}{20}\ln(2x^2 - (\sqrt{5}+1)x + 2)\right) - \left(\frac{\sqrt{5}+1}{20}\ln(2x^2 + (\sqrt{5}-1)x + 2)\right) + \left(\frac{2}{\sqrt{5}}\left(\frac{\arctan\left(\frac{4x-1+\sqrt{5}}{\sqrt{10+2\sqrt{5}}}\right)}{\sqrt{10+2\sqrt{5}}} - \frac{\arctan\left(\frac{4x-1-\sqrt{5}}{\sqrt{10-2\sqrt{5}}}\right)}{\sqrt{10-2\sqrt{5}}}\right)\right) + \text{const.}$
7	$\frac{x^2}{2} + \frac{-\ln(x^2+1) + \frac{\ln(x^4-x^2+1)}{2} - \sqrt{3}\arctan\left(\frac{2x^2-1}{\sqrt{3}}\right)}{6} + \text{const.}$

Each of these types of calculations is useful and will be discussed below. In order to generate the characteristics of the tail, fixed values of Q_2 are selected between 0 and $Q_{2,f}$. One implicit calculation using $T^*(x)$ for $x = 1$ is carried out for each of these values to learn when each characteristic emerges from the column. Then, the point of each characteristic is calculated explicitly using $\Xi(\tau^*, Q_2)$ between 0 and the previously calculated values of $T^*(x)$. The resulting characteristics are shown in Figure 1 as dashed lines.

Careful examination of Figure 1 reveals an interesting phenomenon. The lowest dashed line in Figure 1 is the characteristic of $Q_2 = Q_{2,f}$. Since it is known that the concentration of bound protein above the second disturbance in C_T (upper dotted line) is Q_2 from the origin point $(\tau_f, 0)$ to point K, a family of parallel characteristics exists in the region of Figure 1 labeled "$Q_{2,f}$ plateau." In this region, the value of Q_2 is constant and equal to $Q_{2,f}$ although the value of C_2 changes. This plateau is bordered by the second disturbance in C_T (dotted line), the $Q_{2,f}$ characteristic that departs from the origin (dashed line), and the shock (solid line).

Calculation of the Shock. After point K in Figure 1, the shock begins to curve. Because no analytical expression exists for the shock path, it is necessary to employ a numerical calculation. The velocity of the shock at any point in the time-space plane is given by the expression:

$$u_{sh} = \frac{1}{1+\beta\frac{Q_2}{C_2}}. \qquad (26)$$

A finite difference scheme based on this known shock velocity can be written as follows:

1. Calculate the current value of Q_2 using $\Theta(\tau, x)$. Calculate the current value of C_2 based on the known Q_2 using the SMA isotherm and assuming that $C_1 = C_T$.
2. Define the angle $\omega = \arctan(\beta Q_2/C_2)$.
3. Calculate the finite differences: $\Delta x = \delta\cos(\omega)$ and $\Delta\tau = \delta\sin(\omega) + \Delta x$.

The variable δ is the distance along the shock path that each finite difference moves. It should be selected to be small enough to ensure convergence; 25 to 50 finite differences will typically be sufficient.

Figure 2 shows the shock path of the shock beyond point K as a solid line that consists of two segments. From point K to point L, the bound protein concentration is given by $Q_{2,f}$ although the mobile phase protein concentration C_2 varies along the shock path. After point L, the bound protein concentration decreases monotonically, and the mobile phase protein concentration C_2 increases along the shock as the protein is desorbed by the salt gradient.

Independent Confirmation of the Breakthrough. A second independent method of calculating the breakthrough time of the shock involves carrying out a mass balance. The mass of protein injected into the column may be calculated:

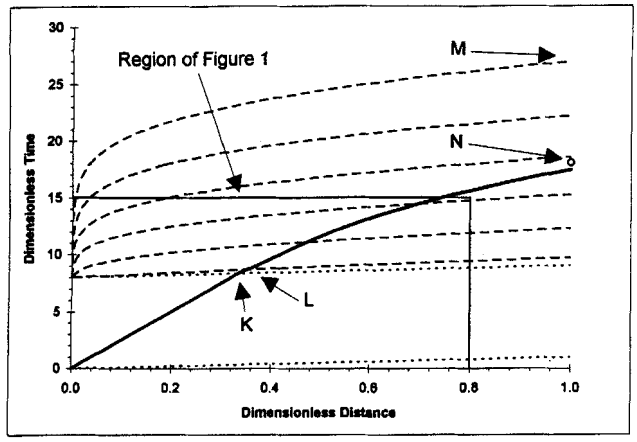

Figure 2. Development plot for gradient chromatography (full view).

Plot includes changes in the value of C_T (dotted lines), the protein front or "shock" (dark solid line), characteristics of the tail (dashed lines), and the estimate of the breakthrough obtained by quadrature applied to Eq. 28 (open circle). Simulation conditions are the same as Figure 1.

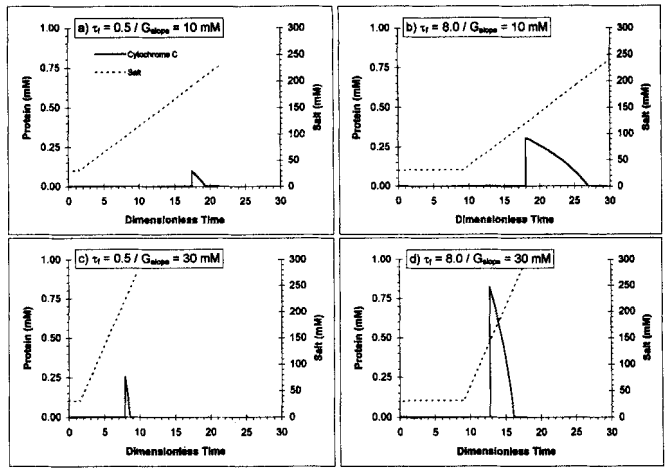

Figure 3. Effect of feed volume and gradient slope.

Simulation conditions: feed: 0.2-mM cytochrome C in 30-mM sodium phosphate, pH 6.0; τ_f and G_{slope}: as indicated on figures.

$$M_{inj} = C_{2,f}\tau_f V_0, \tag{27}$$

where V_0 is the dead volume of the column. As mentioned earlier, the point at which the peak finishes eluting from the column can be calculated using Eq. 19. This point is labeled "M" in Figure 2. If an integration of the mass eluting from the column is carried out, it is expected that the following equation will be satisfied:

$$M_{inj} = V_o\int_{\tau_{bt}}^{\tau_{id}} C_2(y,1)dy = -V_o\int_{\tau_{id}}^{\tau_{bt}} C_2(y,1)dy, \tag{28}$$

where $C_2(\tau,1)$ is the concentration of protein eluting from the end of the column at nondimensional time τ, τ_{bt} and τ_{id} are the nondimensional times at which the protein peak breaks through at the end of the column and at which the protein peak finishes eluting from the column, respectively, and y is a dummy variable of integration. In order to calculate $C_2(\tau,1)$, $Q_2(\tau,1)$ may be calculated using $\Theta(\tau,x)$. Subsequently, C_2 is calculated based on the known Q_2 using the SMA isotherm and assuming that $C_1 = C_T$.

Evaluation of Eq. 28 may be carried out numerically using a method of quadrature such as the trapezoid rule. In Figure 2, the point $(\tau_{bt},1)$ estimated by quadrature applied to Eq. 28 is represented by a circle labeled "N." Comparison of the arrival time of the shock with this circle reveals only slight disagreement between the two methods of calculation. As the number of finite difference points used to calculate the shock path and the number of quadrature points are increased, this disagreement will decrease. However, some disagreement will always remain due to the approximation in which C_T was used as an approximation of C_1.

For a relatively small feed injection, the disagreement between the breakthrough time (τ_{bt}) calculated by integration along the shock path and the breakthrough time calculated by integration of the peak mass remains small. For an injection of 0.5 column dead volumes of 0.2 mM cytochrome C with an initial counterion concentration of 30 mM and a gradient slope of 10 mM per column volume (Figure 3a), the breakthrough time calculated by integration along the shock path is 17.42 (using 100 finite differences) and the breakthrough time calculated by integration of the peak mass is 17.45 (using 100 finite differences). Clearly, good agreement is achieved using a relatively small number of finite differences under these conditions.

On the other hand, the convergence of the two methods is not quite as close for large feed injections. In Table 2, the estimation of the breakthrough time for a feed injection of 8.0 column dead volumes (Figure 3b) is considered. As the number of finite differences used in the calculation of the shock path is doubled from 29 to 57, and subsequently to 113 and 226, the breakthrough time converges linearly toward a value of 17.39 (calculated by extrapolation of the linear trend). In contrast, the technique of integration over the mass of the peak converges toward 17.96, a value of 3% larger than the value obtained by the first method. Both methods are nevertheless useful, each having a separate region of the solution in which it would be expected to be most accurate. If the shock path is short (i.e., when loading is heavy, saturating most of the column's length), then the accumulated error in calculation of the breakthrough time will be small. In that case, integration along the shock path will be the preferred method. In contrast, as the shock path becomes longer, the accumulation of error is greater, and integration along the

Table 2. Convergence of the Two Estimates of the Breakthrough Time

Integrating Shock Path			Mass Balance Over Peak		
Finite Diff.	τ_{bt}	$\Delta\tau_{bt}$	Finite Diff.	τ_{bt}	$\Delta\tau_{bt}$
29	17.564	—	25	18.304	—
57	17.482	−0.082	51	18.132	−0.172
113	17.436	−0.047	103	18.046	−0.086
226	17.411	−0.025	207	18.003	−0.043

*Finite differences along the shock path calculation from point K in Figure 2 to end of column.

shock path is the less accurate method. It has been the observation of the authors that, for most preparative-size injections, the shock path is long enough to make conducting a mass balance the preferred method.

Experimental Studies

Materials

Sodium monobasic phosphate, sodium dibasic phosphate, and cytochrome C were purchased from Sigma Chemical (St. Louis, MO). Sodium chloride was purchased from Aldrich Chemical (Milwaukee, WI). Phosphoric acid was purchased from Fisher Scientific (Rochester, NY). The strong cation exchange column employed in this work (sulfonate exchange groups on a polystyrene/divinyl benzene backbone, 15 μm, 54×5 mm ID) was a gift from Pharmacia Biotech AS (Lilistrom, Norway). POROS R/H reversed phase chromatographic column (100×4.6 mm ID) was purchased from PerSeptive Biosystems (Cambridge, MA).

Apparatus

The chromatograph employed in this work consisted of two Model P-500 pumps (Pharmacia, LKB, Uppsala, Sweden) connected to the chromatographic column via a Model MV-7 injector (Pharmacia, LKB). During parameter estimation, the column effluent was monitored using a Model 757 Spectroflow UV-VIS absorbance detector (Applied Biosystems, Foster City, CA) and a Powermate 2 personal computer (NEC Inc., Tokyo, Japan) running Maxima 820 data-collection software (Waters Chromatography Division, Millipore Corp.). During gradient experiments, fractions of the column effluent were collected directly from the column using Model 2212 Helirac fraction collector (Pharmacia, LKB). During fraction analysis, a Spectroflow 757 UV-VIS absorbance detector (Applied Biosystems) was employed to monitor the column effluent, and a model C-R3A Chromatopac integrator (Shimadzu, Kyoto, Japan) was employed for data acquisition and analysis.

Procedures

Parameter Estimation. The estimation of the SMA equilibrium parameters that appear in Table 3 has been discussed previously (Gadam et al., 1993; Gallant et al., 1995a). In order to employ the model described earlier, it is necessary that the characteristic charge of the protein be an integer. This

Table 3. Parameters Employed in Simulations*

Component	Characteristic Charge (ν_i)	Steric Factor (σ_i)	Equilibrium Constant (K_{1i})
Counter Ion			
Sodium Ion	1.00	0.00	1.00
Protein			
Cytochrome-C	5.67	27.4	4.50×10^{-2}
Cytochrome-C†	6.00	26.59	3.19×10^{-2}

*Column: 54×5 mm ID; column capacity (Λ): 525 mM; void fraction (ϵ): 0.728.
†Indicates best-fit values of SMA parameters for that protein with ν_i restricted to an integer value.

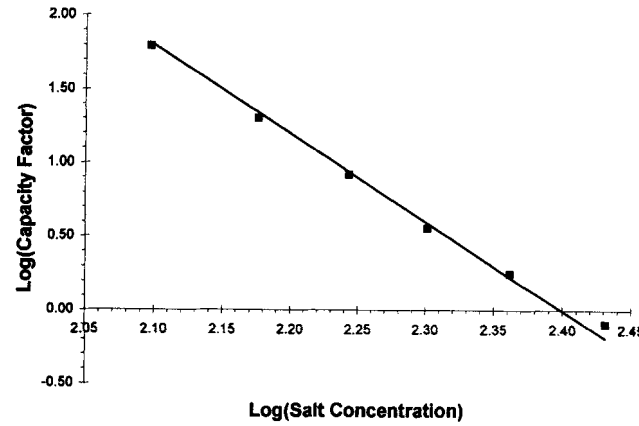

Figure 4. Log(k') vs. log(salt concentration) plot.
Symbols (■) represent data taken under infinite dilution conditions, sodium phosphate buffer, pH 6.0; line is SMA representation of data for integral value of characteristic charge.

does not present a significant restriction on the validity of the solution as will be seen below.

In order to estimate the characteristic charge ν_2 and equilibrium constant K_{12} of the protein, linear elution experiments were conducted at various mobile-phase salt concentrations. The resulting data were fit to the following linearized equation (Gadam et al., 1993):

$$\log(k_2') = \log(\beta K_{12}\Lambda^{\nu_2}) - \nu_2 \log(C_1). \tag{29}$$

This fitting procedure provided two estimates of the characteristic charge ν_2 and equilibrium constants K_{12} of the protein. The first estimate is an unrestricted estimate of ν_2 and K_{12}; the second estimate is restricted to an integer value of ν_2. Both estimates are given in Table 3. The integer value of ν_2 and the corresponding value of K_{12} were employed in Figure 4 to describe the linear adsorption data. As can be seen in the figure, the restriction on ν_2 did not prevent the model from accurately representing these data.

In order to estimate the steric factor σ_2, nonlinear frontal experiments were carried out over a range of mobile-phase salt concentrations (Gadam et al., 1993; Gallant et al., 1995a).

$$C_{2,\mathrm{SMA}} = \left(\frac{C_{1,f}}{\Lambda - (\nu_2 + \sigma_2)Q_{2,f}}\right)^{\nu_2} \frac{Q_{2,f}}{K_{12}}. \tag{30}$$

Equation 30 was used in conjunction with the experimental protein isotherms in order to estimate the steric factors σ_2. The residuals between the experimental protein concentration ($C_{2,f}$) and the estimate of the protein concentration ($C_{2,\mathrm{SMA}}$) obtained from Eq. 30 may be calculated as a function of the steric factor. Minimization of the sum of squares of the residuals using a Newton–Raphson technique established the estimated steric factor. As can be seen in Figure 5, the restriction on ν_2 did not prevent the model from accurately representing the nonlinear data.

Linear Gradient Chromatography. For the linear gradient experiments, Buffer A consisted of a 30-mM sodium phosphate solution pH 6.0. Buffer B contained 470 mM sodium chloride in a 30-mM sodium phosphate buffer, pH 6.0. The

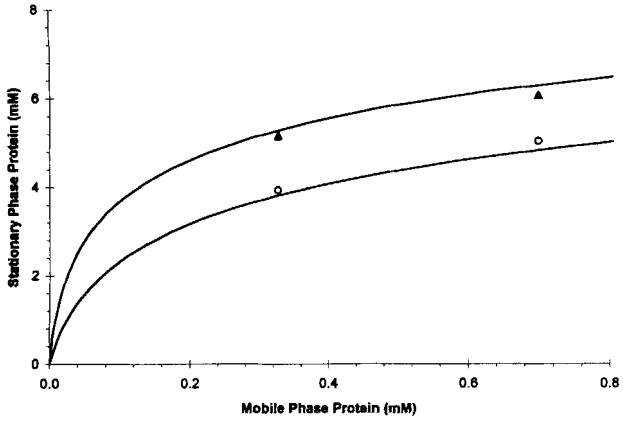

Figure 5. Experimental isotherm and SMA representation.

Experimental isotherm points taken at 125-mM (▲) and 150-mM (○) sodium ion concentration, sodium phosphate buffer, pH 6.0. Lines are SMA representation of data for integral value of characteristic charge.

protein was dissolved in Buffer A and loaded into a 10-mL injection loop. Following equilibration of the column with Buffer A, the feed solution was introduced into the column. After an appropriate feed volume was loaded, the linear gradient was initiated. The gradient program was timed so that the mobile phase salt concentration at the column inlet would begin to rise immediately after the injection, as described by the boundary conditions (Eqs. 5 and 6). Fractions of the column effluent were collected and analyzed for protein concentration using the procedure described below.

Protein Analysis. Analysis of the fractions collected during linear gradient operation was performed by ion-exchange high-performance liquid chromatography (HPLC) under isocratic conditions using mobile phase of 50-mM sodium phosphate and 110-mM sodium chloride, pH 6.0. The fractions were diluted 5- to 100-fold. Protein peaks were detected using a UV-VIS detector set to 280 nm. The compositional data from the protein analysis were used to generate a histogram representing each linear gradient experiment.

Results and Discussion

The method of characteristics can be readily employed to generate the effluent profile in preparative linear gradient chromatography. Three categories of chromatograms may result from the development plots described earlier. If the peak elutes from the column after the points K and L of Figure 2 have been reached within the column, a shark fin-shaped gradient peak will emerge. Such a peak is shown in Figure 6a. If point K has been reached inside the column but not point L, then there will be a steep ramp up as the peak emerges from the column (rather than a pure shock), Figure 6b. If neither point K nor point L is reached inside the column, a peak with a plateau followed by a ramp up will emerge from the column, Figure 6c. Assuming that all the operating conditions have been held constant except feed volume, Figures 6a, 6b, and 6c represent progressively larger feed volumes.

Under typical operating conditions of gradient chromatography, the loadings are not high enough for either Figure 6b or Figure 6c to be reached inside the column. As feed loadings increase in preparative gradient chromatography, they pass from the infinite dilution regime to a regime of nonlinearity resulting in asymmetric peaks as shown in Figure 3a. During the simulated loading for this figure, approximately 2% of the column length is occupied by protein. Although the protein concentration is relatively high during loading, 0.2 mM, significant dilution of the feed would not significantly alter the loading length due to the extreme nonlinearity of the protein isotherm under low salt concentrations. Further increasing the feed load is generally desirable in order to purify large amounts of protein in each cycle. Figure 3b represents a substantial injection in which about 35% of the column length is occupied by protein during the feed cycle. (The development plot for this loading is seen in Figures 1 and 2.) Depending on the resolution between the product and other contaminating impurities, it may be possible to increase the gradient slope and reduce the time required to accomplish the separation. In Figure 3c and Figure 3d, the effect of increasing gradient slope is seen.

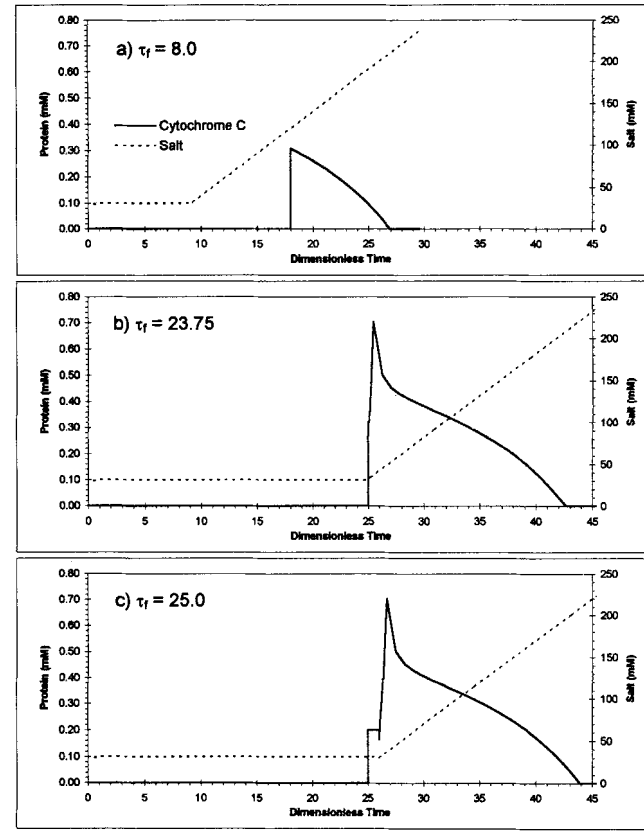

Figure 6. Three categories of gradient chromatograms.

Simulation conditions: feed: 0.2-mM cytochrome C in 30-mM sodium phosphate, pH 6.0; τ_f: as indicated on figure parts.

Having examined the behavior of gradient chromatography of a pulse of finite width and height, the model will now be tested against gradient experiments conducted with the protein cytochrome C. Figure 7 presents a gradient chromatogram in which a large mass of cytochrome C has been loaded onto the column and subsequently eluted using a gradient of 30 mM per dimensionless time unit (30 mM per column dead volume). The simulated sodium ion concentration in the column effluent is shown as a dotted line. The experi-

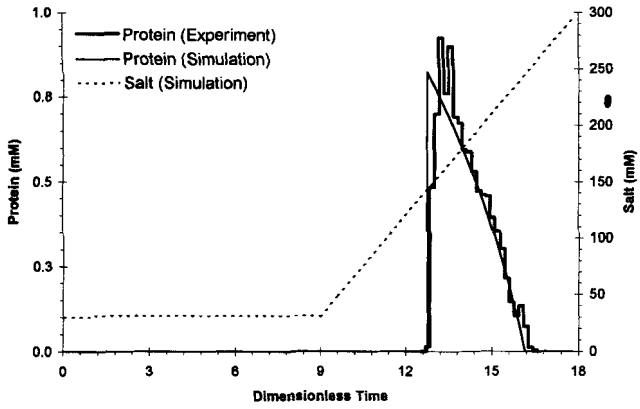

Figure 7. Comparison of simulated and experimental chromatograms.

Comparison of simulated and experimental chromatograms: (a) Reconstructed experimental linear gradient chromatogram. Feed Injection: 8.0 dimensionless time units of 0.20-mM cytochrome C in 30-mM sodium phosphate. Gradient Slope: 30-mM sodium ion concentration per dimensionless time unit. Operating Conditions: 0.5 mL/min, pH 6.0, 125 μL fractions. (b) Simulated chromatogram.

mental cytochrome C histogram is shown using a dark solid line. The high protein concentration necessitated the use of fraction collection because no wavelength could be found that provided a linear detector response. As can be seen in the figure, the model (light solid line) accurately predicts the breakthrough time and the forward arc of the overloaded peak.

The gradient slope was subsequently lowered to 10-mM sodium ion concentration per dimensionless time unit. At this gradient slope, the cytochrome C peak required substantially more time to elute from the column. The experimental and simulated chromatograms are shown in Figure 8. The cytochrome C peak is shown as a dark solid line, and the simulated peak is shown as a light solid line. Again, the model accurately predicts the elution behavior of the protein.

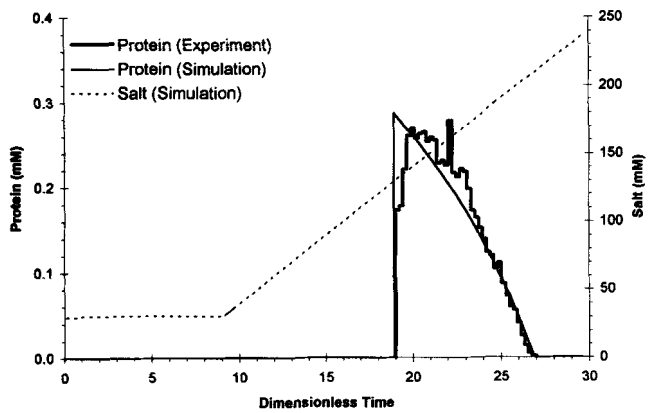

Figure 8. Comparison of simulated and experimental chromatograms.

Comparison of simulated and experimental chromatograms: (a) Reconstructed experimental linear gradient chromatogram. Feed Injection: 8.0 dimensionless time units of 0.17-mM cytochrome C in 30-mM sodium phosphate. Gradient Slope: 10-mM sodium ion concentration per dimensionless time unit. Operating Conditions: 0.5 mL/min, pH 6.0, 167 μL fractions. (b) Simulated chromatogram.

Conclusions

The focus of this work has been on understanding the gradient elution of a single protein in ion-exchange chromatography. Of course, the most important application of this understanding is to multicomponent chromatographic separations. In preparative gradient chromatographic separations, both differential elution and differential migration play important roles (Coffman et al., 1994). (*Differential elution* may be defined as the movement of a single product or impurity through the column while all other products or impurities are bound strongly to the stationary phase. *Differential migration* is the movement of more than one component through the column at the same moment.)

Differential migration plays a more important role in preparative gradient chromatography than in analytical gradient chromatography. While the development path of a protein band in analytical chromatography may be seen as a single line in the x-τ plane, the development path of a protein band in preparative chromatography is represented by a region of the development plot (Figure 2). Preparative separation of a multicomponent feed stream results in several overlapping regions in the x-τ plane representing the product and the impurities. A successful separation allows the product region to emerge from the column with a minimum of contamination (overlap) with the impurities. In order to maximize chromatographic productivity, it is critically important to understand the role of nonlinear adsorption in dictating the shape of product and impurity zones in the development plot.

The ability to rapidly consider the effects of nonlinear adsorption in gradient elution chromatography using a spreadsheet represents a powerful tool for methods development in preparative ion-exchange chromatography. Although the model presented here does not account for dispersion, comparison of the predictions of this model with a dispersion model (Gibbs and Lightfoot, 1986; Frey, 1990; Carta and Stringfield, 1992) will make it evident whether the thermodynamics of adsorption or dispersion effects are more important for a particular separation. Further, since both types of models require similar (though not identical) parameter estimation experiments, their use in a complementary fashion is quite convenient. Of course, solution of the full problem including dispersion, nonlinear adsorption, and multicomponent competitive binding is possible using numerical methods (Yamamoto et al., 1983a,b; Antia and Horváth, 1989; Snyder et al., 1991; Gu et al., 1992; Bellot and Condoret, 1993; Whitley et al., 1994).

Acknowledgments

This research was funded by Pharmacia Biotech and from the National Science Foundation, Grant no. CTS-9416921.

Notation

$C_{i,f}$ = feed concentration, mM
F_i = function that returns Q_i when given C_1, ..., C_{NC}, mM
H = height equivalent to a theoretical plate, cm
k' = infinite dilution capacity factor $[k' = (t_R - t_0)/t_0]$
L = column length, cm
M_{inj} = mass of protein injected, μmol
NC = number of components present in mobile phase

$\hat{Q}_{1i}$ = bound salt that is sterically shielded by component i, mM
t = time, s
t_R = retention time, s
t_0 = column dead time, s
U = velocity, cm/s
u_0 = chromatographic velocity, $u_0 = u_s/\epsilon$, cm/s
V_{col} = empty column volume, mL
V_f = feed volume, mL
V_{sp} = stationary phase volume ($V_{sp} = (1 - \epsilon)V_{col}$), mL
X = axial position in column, cm

Greek letters

Δ = change in a variable across a discontinuity
ϵ = total porosity of column
Θ = function that gives Q_2 along a particular characteristic when supplied with x and τ^*
Λ = column capacity for a monovalent salt counterion, mM
Ξ = function that gives x along a particular characteristic when supplied with τ^* and Q_2
T* = function that gives τ^* along a particular characteristic when supplied with x and Q_2

Subscript

i = mobile/stationary phase component number ($i = 1$ designates salt)

Literature Cited

Antia, F. D., and C. Horváth, "Gradient Elution in Non-Linear Preparative Liquid Chromatography," *J. Chromatog.*, **484**, 1 (1989).

Bellot, J. C., and J. S. Condoret, "Theoretical Study of the Ion-Exchange Preparative Chromatography of a Two-Protein Mixture," *J. Chromatog.*, **635**, 1 (1993).

Boardman, N. K., and S. M. Partridge, "Separation of Neural Proteins on Ion-Exchange Resins," *Biochem. J.*, **59**, 543 (1955).

Brooks, C. A., and S. M. Cramer, "Steric Mass-Action Ion-Exchange: Displacement Profiles and Induced Salt Gradients," *AIChE J.*, **38**, 1969 (1992).

Carta, G., and W. B. Stringfield, "Analytical Solution for Volume-Overloaded Gradient Elution Chromatography," *J. Chromatog.*, **605**, 151 (1992).

Coffman, J. L., D. K. Roper, and E. N. Lightfoot, "High-Resolution Chromatography of Proteins in Short Columns and Adsorptive Membranes," *Bioseparation*, **4**, 183 (1994).

Czok, M., and G. Guiochon, "The Physical Sense of Simulation Models of Liquid Chromatography," *Anal. Chem.*, **62**, 189 (1990a).

Czok, M., and G. Guiochon, "Comparison of the Results Obtained with Different Models for the Simulation of Preparative Chromatography," *Comput. Chem. Eng.*, **15**, 1435 (1990b).

de Bokx, P. K., P. C. Baarslag, and H. P. Urbach, "Modeling of Displacement Chromatography Using Non-Ideal Isotherms," *J. Chromatog.*, **594**, 9 (1992).

Drager, R. R., and F. E. Regnier, "Application of the Stoichiometric Displacement Model of Retention to Anion-Exchange Chromatography of Nucleic Acids," *J. Chromatog.*, **359**, 147 (1986).

Frey, D. D., "Asymptotic Relations for Preparative Gradient Chromatography of Biomolecules," *Biotechnol. Bioeng.*, **25**, 1055 (1990).

Gadam, S. D., S. R. Gallant, and S. M. Cramer, "Transient Profiles in Ion-Exchange Displacement Chromatography," *AIChE J.*, **41**, 1676 (1995).

Gadam, S. D., G. Jayaraman, and S. M. Cramer, "Characterization of Non-Linear Adsorption Properties of Dextran-Based Polyelectrolyte Displacers in Ion-Exchange Systems," *J. Chromatog.*, **630**, 37 (1993).

Gallant, S. R., A. Kundu, and S. M. Cramer, "Modeling Nonlinear Elution of Proteins in Ion-Exchange Chromatography," *J. Chromatog.*, **702**, 125 (1995a).

Gallant, S. R., A. Kundu, and S. M. Cramer, "Optimization of Step Gradient Separations: Consideration of Nonlinear Adsorption," *Biotechnol. Bioeng.*, **47**, 355 (1995b).

Gallant, S. R., S. Vunnum, and S. M. Cramer, "Optimization of Preparative Ion-Exchange Chromatography: Linear Gradient Separations," *J. Chromatog.*, **725**, 295 (1996).

Gerstner, J. A., and S. M. Cramer, "Cation-Exchange Displacement Chromatography of Proteins with Protamine Displacers," *Biotechnol. Prog.*, **8**, 540 (1992a).

Gerstner, J. A., and S. M. Cramer, "Heparin as a Nontoxic Displacer for Anion-Exchange Protein Displacement Systems," *BioPharm*, **5**, 42 (1992b).

Gibbs, S. J., and E. N. Lightfoot, "Scaling Up Gradient Elution Chromatography," *Ind. Eng. Chem. Fundam.*, **25**, 490 (1986).

Gu, T., Y. Truei, G. Tsai, and G. Tsao, "Modeling of Gradient Elution in Multicomponent Nonlinear Chromatography," *Chem. Eng. Sci.*, **47**, 253 (1992).

Helfferich, F., and G. Klein, *Multicomponent Chromatography*, Marcel Dekker, New York (1970).

Hildebrand, F. B., *Advanced Calculus for Applications*, Prentice Hall, Englewood Cliffs, NJ (1976).

Jayaraman, G., S. D. Gadam, and S. M. Cramer, "Ion-Exchange Displacement Chromatography of Proteins: Dextran-Based Polyelectrolytes As High Affinity Displacers," *J. Chromatog.*, **630**, 53 (1993).

Li, Y., and N. Pinto, "Model for Ion-Exchange Equilibria for Macromolecules in Preparative Chromatography," *J. Chromatog.*, **702**, 113 (1994).

Ma, Z., and G. Guiochon, "Application of Orthogonal Collocation on Finite Elements in the Simulation of Non-Linear Chromatography," *Comput. Chem. Eng.*, **15**, 415 (1991).

Parente, E. S., and D. B. Wetlaufer, "Relationship Between Isocratic and Gradient Elution in High Performance Ion-Exchange Chromatography of Proteins," *J. Chromatog.*, **333**, 29 (1986).

Rhee, H. K., R. Aris, and N. R. Amundson, *First-Order Partial Differential Equations*, Vol. I, Prentice Hall, Englewood Cliffs, NJ (1986).

Snyder, L. R., *High-Performance Liquid Chromatography— Advances and Perspectives*, C. Horváth, ed., Academic Press, New York, p. 208 (1980).

Snyder, L. R., J. W. Dolan, and G. B. Cox, "Optimum Experimental Conditions for Heavily Overloaded Separations," *J. Chromatog.*, **540**, 21 (1991).

Velayudhan, A., "Studies in Nonlinear Chromatograhy," PhD Diss., Yale Univ., New Haven, CT (1990).

Velayudhan, A., and C. Horváth, "Preparative Chromatography of Proteins Analysis of the Multivalent Ion-Exchange Formalism," *J. Chromatog.*, **443**, 13 (1988).

Wankat, P. C., *Rate Controlled Separations*, Elsevier, London (1990).

Whitley, R. D., R. Wachter, F. Liu, and N. H. L. Wang, "Ion-Exchange Equilibria of Lysozyme, Myoglobin, and BSA," *J. Chromatog.*, **465**, 137 (1989).

Whitley, R. D., X. Zhang, and N. H. L. Wang, "Protein Denaturation in Nonlinear Isocratic and Gradient Chromatography," *AIChE J.*, **40**, 1067 (1994).

Yamamoto, S., K. Nakanishi, R. Matsuno, and T. Kamikubo, "Ion Exchange Chromatography of Proteins Prediction of Elution Curves and Operating Conditions: I. Theoretical Considerations," *Biotechnol. Bioeng.*, **25**, 1465 (1983a).

Yamamoto, S., K. Nakanishi, R. Matsuno, and T. Kamikubo, "Ion Exchange Chromatography of Proteins Prediction of Elution Curves and Operating Conditions: II. Experimental Verification," *Biotechnol. Bioeng.*, **25**, 1373 (1983b).

Yamamoto, S., M. Nomura, and Y. Sano, "Adsorption Chromatography of Proteins: Determination of Optimum Conditions," *AIChE J.*, **33**, 1426 (1987).

Manuscript received Aug. 25, 1995, and revision received Dec. 27, 1995.